JOURNAL OF MATERIALS SCIENCE **39** (2004) 3281–3292

Micromechanical properties in lamellar heterophase polymer systems

G. H. MICHLER, R. ADHIKARI, S. HENNING
Department of Engineering, Institute of Materials Science, Martin Luther University Halle-Wittenberg, D-06099 Halle/Saale, Germany
E-mail: michler@iw.uni-halle.de

Several nanoanalytical techniques based on electron and atomic force microscopy were used to analyse the micromechanical deformation mechanisms in different nanostructured lamellae forming heterogeneous polymers: in (semicrystalline) β-modified isotactic polypropylenes and (amorphous) lamellar styrene/butadiene block copolymers. It was found that the deformation processes in these two entirely different classes of materials are governed by fundamentally similar mechanisms due to similar dimension and arrangement of the nanostructures. The basic mechanism shows two steps: The initial step is determined by a plastic deformation of the soft (amorphous or rubbery) phase with a reorganisation of the hard (crystalline or glassy) lamellae and their orientation towards the deformation direction. The second step is characterised by the intense plastic deformation (yielding) of the hard lamellae up to elongations of several 100%.

1. Introduction

Polymeric materials possess a rich variety of structural diversities. While the molecular and macromolecular architecture determines some fundamental properties of the polymers (e.g., thermal behaviour, chemical properties etc.), the fabrication and post-fabrication history greatly influences their morphology and final mechanical behaviour. Therefore, it is of tremendous practical importance to control the supermolecular structures or morphology of the materials. However, not all of the manifold structural or morphological details influence the ultimate mechanical properties to the same extent. There are details that play a dominating role in determining their properties, i.e., the so called *properties determining structures* [1]. The influence of these structural details on the mechanical properties is determined by the micromechanical processes, which appear under the action of applied load. There is a large variety of micromechanical processes of deformation and fracture depending on the morphological details of polymers and the loading conditions. These processes occur on mesoscopic, microscopic and nanometer scales inside a material and include not only movements on the macromolecular level such as reptation, stretching and scission of the macromolecules but also the microscopic phenomena including microyielding, microcavitation and formation of crazes, shear bands or deformation zones, and, finally, the mesoscopic phenomena ranging from crack initiation and propagation to the ultimate macroscopic fracture of the specimens. These processes define the *micromechanical properties* of the polymers or the *micromechanics* [1, 2].

Improved knowledge of micromechanical properties allows us a deeper insight into the interrelation between the property determining structures and the ultimate properties, i.e., it enables a precise understanding of the structure-property correlations. Such a detailed knowledge of structure-property correlations opens up a defined modification of the morphology for attaining the properties desired for practical applications. This was named *microstructural construction of polymers* [1, 2]. Comparison of micromechanical processes in different polymeric materials may reveal new information that enable us to find new possibilities for an additional improvement of mechanical properties. Transferring such new mechanisms from microstructurally constructed model polymers to technologically important materials by a defined scaling-up process could be helpful to come finally to new classes of polymers.

Following this concept, in this work micromechanical processes of different classes of heterogeneous polymers with a comparable microstructure—semicrystalline β-modified isotactic polypropylenes and styrene/butadiene block copolymers—are studied using techniques of transmission electron microscopy (TEM), scanning electron microscopy (SEM) and scanning force microscopy (SFM). The bridge between both classes of polymers is a similar lamellar nanostructure with ordered crystalline lamellae and amorphous interlamellar layers in β-iPP and alternating polystyrene (PS) and polybutadiene (PB) lamellae in the block copolymers.

Isotactic polypropylene (iPP) belongs to the family of commodity plastics and occupies the third place after low density polyethylene (LDPE) and poly(vinyl chloride) (PVC) in the worldwide plastic market [3]. The most important applications of this polymer are in several fields of everyday life, as in the production of

films, textile fibres and moulded parts. The plastic is processed mainly by extrusion and injection moulding. The pronounced diversity of this polymeric material is also connected with the existence of several crystal modifications. Of particular interest from the technical point of view is the β-modification of iPP because of its enhanced toughness compared to the ordinary α-modification [4, 5].

Block copolymers are a subject of enormous academic and industrial interest. The reason for this interest is the ability of block copolymer molecules to self-assemble into a variety of nanostructures [6–9]. These materials allow a precise control of mechanical properties through the variation of easily accessible nanostructures (often called microphase separated structures) formed by intramolecular phase separation. In general, the type of microphase separated morphology to be formed is determined by the relative volume fraction of the components. However, modification of the architectural structure (type of interface, chain topology, symmetry of the blocks etc.) of the block copolymers leads to a new balance in the effective volume fraction of the component chains and finally determines the kind of morphology [7–13].

2. Experimental

2.1. Materials used

Materials of two different classes of lamellae forming heterogeneous polymers were chosen: semicrystalline isotactic polypropylene in α- (α-iPP) and in β-form (β-iPP) and amorphous styrene/butadiene block copolymers, see Table I. The structure and morphology of the samples used are illustrated schematically in Fig. 1.

The α- and β-nucleated isotactic polyprophylene samples were supplied by Borealis AG, Linz. The β-modified material was prepared using a plate press following a special multistage crystallisation process, and it is considered to contain exclusively the β-crystalline form of iPP.

The block copolymers, a linear triblock (SBS-Ln) and a star block copolymer (SBS-St) were prepared by sequential anionic polymerisation (provided by the BASF Aktiengesellschaft). The samples were cast from neutral solvent toluene and annealed at 120°C under vacuum for 48 h in order to allow the formation of a well ordered morphology. Some of the samples were also produced by injection moulding (mass temperature 250°C and mould temperature 45°C).

TABLE I Characteristics of the samples used in this study

Sample code	M_w (kg/mol)	M_w/M_n	Molecular structure, morphology
α-iPP	~400	~7.00	Non-nucleated iPP, cross-hatched lamellae
β-iPP	~400	~7.00	β-nucleated iPP, lamellar crystalline morphology
SBS-Ln	108	1.17	Asymmetric linear block copolymer with tapered transition; lamellar morphology, details in [13]
SBS-St	174	1.69	Asymmetric star block copolymer with lamellar morphology, details in [13, 29]

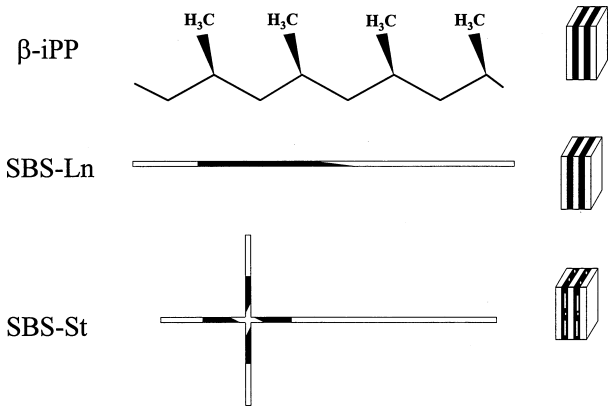

Figure 1 Scheme showing the molecular structure and morphology of the samples studied; white and dark areas in morphology schemes correspond to hard and soft phases, respectively.

2.2. Techniques

Several techniques have been used to investigate the morphology, mechanical properties and micromechanical processes of the polymeric materials.

Morphology (supermolecular structure) was studied using ultramicrotomed ultrathin sections after selective staining with osmium tetroxide (OsO_4) or ruthenium tetroxide (RuO_4) and inspection in a 200 kV—transmission electron microscope (TEM, Jeol). Solution cast thin films and cryo-ultramicrotomed faces of the bulk materials were used for scanning force microscopic (SFM, Digital Instruments) investigations.

Mechanical properties of the samples were characterised by uniaxial tensile testing at room temperature (23°C).

Miniaturised tensile bars of iPP were punched out of 1 mm thick pressure plates using a special piercing tool and deformed with a traverse speed of 1 mm/min in a miniature materials tester (Minimat, Polymer Laboratories, UK).

The tensile behaviour of the injection moulded or solution cast block copolymer samples was determined using a universal tensile machine (Zwick 1425) with a cross head speed of 50 mm/min.

Micromechanical properties have been investigated using two different techniques:

- *Characterisation of deformed bulk materials*: From the strained samples with strain induced structural changes inside, thin sections have been prepared and investigated by TEM and SFM. Additionally, the ultramicrotomed faces of the bulk samples have been investigated by SFM and scanning electron microscopy (SEM, Jeol). The iPP samples were etched following the permanganic etching procedure according to Olley and Basset [14].
- *In situ microscopic techniques*: Scanning electron microscope (SEM), scanning force microscope (SFM) and high voltage transmission electron

microscope (HVEM) in combination with special miniaturised stretching devices have been used to monitor the development of deformation structures in thin polymer films (thickness ranging from 50 nm to a few microns prepared by cryo-ultramicrotomy).

SFM is successfully used to monitor the local structural changes in the polymers but the information is limited to the surface and sub-surface regions. Although this method allows a morphological characterisation of the polymer surface from a few nanometers up to a few hundred micrometers in lateral dimension with the same scanning probe, in many cases the information may not be representative of the bulk material. Semithin sections (thickness a few hundred nanometers to a few micrometers; showing a good mechanical stability and revealing deformation structures which are more representative of the bulk specimens) were used for the investigation by HVEM and SEM.

Macromolecular orientation processes have been studied using Fourier transform infrared (FTIR) spectroscopy of deformed samples (rheo-optical method). Changes in the absorption intensity of representative bands of the different polymeric phases during deformation yield information about the molecular orientation of these individual phases. The theoretical background of this method is discussed elsewhere [15–17].

FTIR measurements were carried out at room temperature using a Perkin Elmer S2000 spectrometer. The investigated samples were prepared by thermal pressing and had dimensions of 20 mm × 10 mm × 0.05 mm.

For the quantitative characterization of molecular orientation of polypropylene during uniaxial stretching, the 998 and 974 cm^{-1} absorption bands have been selected. The 998 cm^{-1} band corresponds to the crystalline phase, while the 974 cm^{-1} band contains contributions of both the amorphous and crystalline phase; the transition moment angle for both these bands is 18° [18]. As the spectrum of PP does not contain any suitable band corresponding to the purely amorphous phase, the orientation of the chains in amorphous phase (f_{am}) can be calculated from the orientation of chains in crystalline phase (f_c at 998 cm^{-1}) and that in the average region (f_{av} at 974 cm^{-1}) [19]. In the case of SBS block copolymers, the absorption bands at 967 and 1069 cm^{-1} were selected for butadiene and styrene phases, respectively. According to the group theory [15], the transition moment angle of the respective bands is assumed to be about 90°.

3. Results

3.1. Morphology and micromechanical processes of iPP

3.1.1. Morphology

Among various crystal modifications in iPP, the α-form is the most frequent and stable crystal modification. Its spherulitic superstructure consists of radially arranged mother lamellae emerging from the spherulite centre, and the daughter lamellae which grow epitaxially at an angle of about 81° to these radial lamellae [20]. The crystalline morphology is characterised by a so called 'cross-hatched' structure and represents an interwoven composite structure dispersed in a mobile amorphous phase, Fig. 2a. The thickness of crystalline lamellae and the lamellar long period is 10–20 nm and 18–30 nm, respectively.

The β-modification represents a metastable phase of the iPP and possesses a lower packing density. The lamellae in the β-iPP propagate radially from the spherulite centre. The interwoven network of the crystallites as observed in the α-form of iPP (Fig. 2a) is not found (see Fig. 2b). The lamellar morphology of the β-nucleated iPP is demonstrated also by the TEM image given in Fig. 3. The special arrangement of the

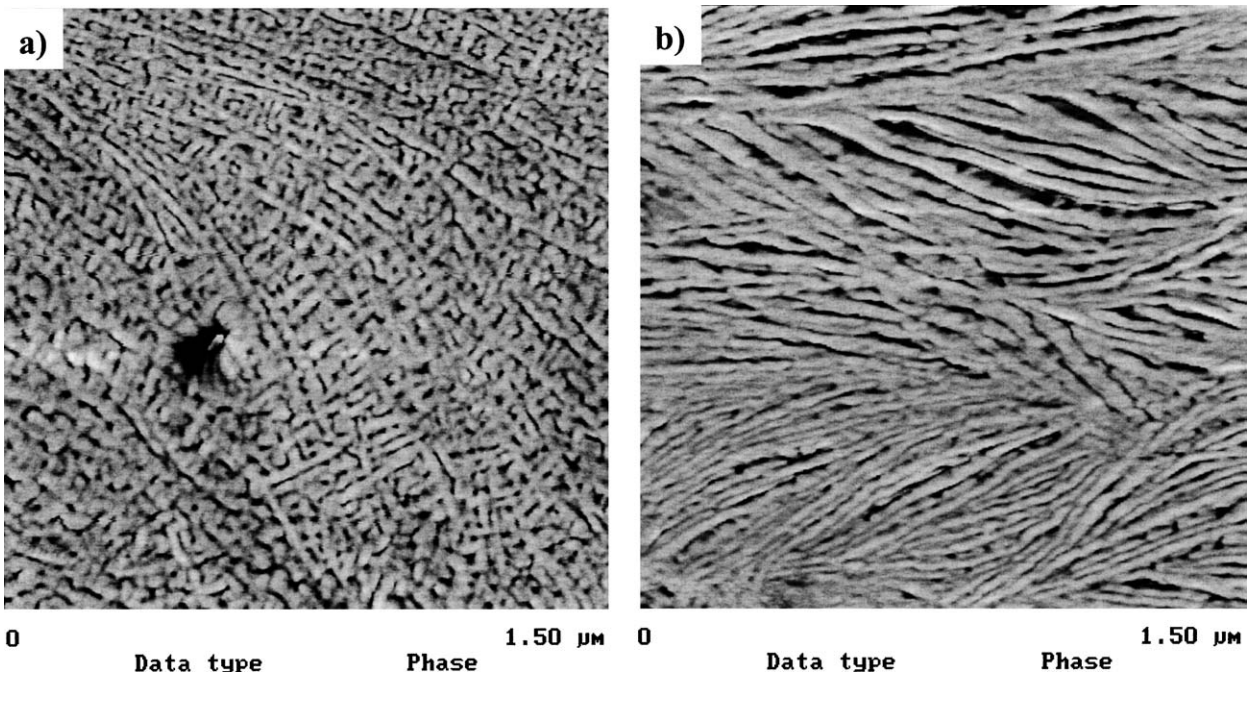

Figure 2 AFM phase images showing the typical morphology of (a) α-iPP and (b) β-iPP .

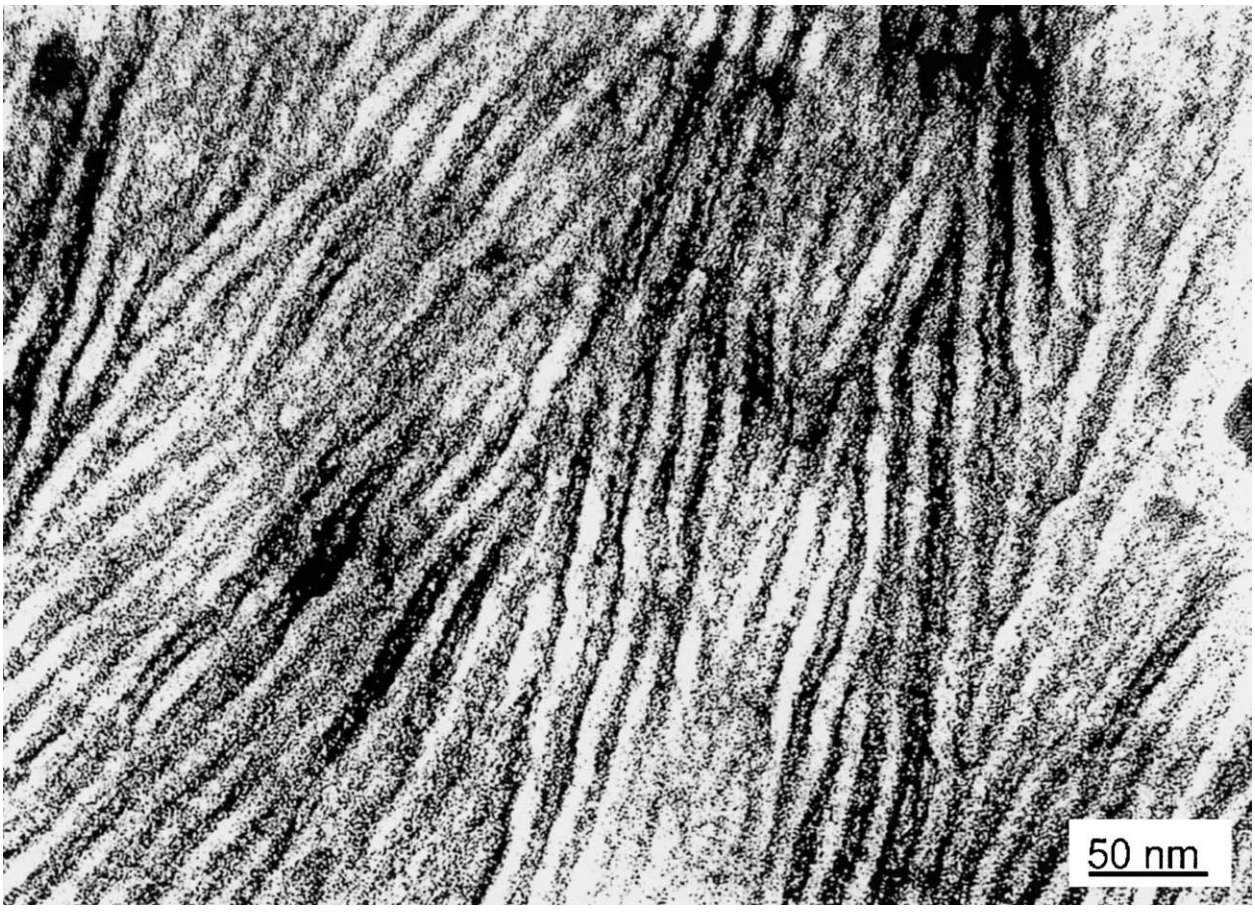

Figure 3 TEM micrograph showing in detail the morphology of β-iPP; RuO_4 staining causes the less denser amorphous phase to appear dark.

crystalline lamellae and interlamellar amorphous material in a parallel manner (stacks) can be interpreted as a lamellar nanostructure (10. . .20 nm) consisting of soft (amorphous) and hard (crystalline) components that are interconnected by tie molecules and entanglements.

3.1.2. Mechanical properties

Stress-strain curves of α- and β-polypropylene samples are presented in Fig. 4. It is clearly noticed that the yield stress of β-iPP is significantly lower than that of the α-modification. Further, the tensile deformation of the β-modification is characterised by a homogeneous stretching of the specimen. In contrast, the deformation of α-modification is accompanied by a pronounced necking and drawing of the specimen.

It has been demonstrated that β-iPP has a higher fracture toughness than the α-iPP [4, 5]. This correlates with the larger area below the stress-elongation curve (cf. Fig. 4).

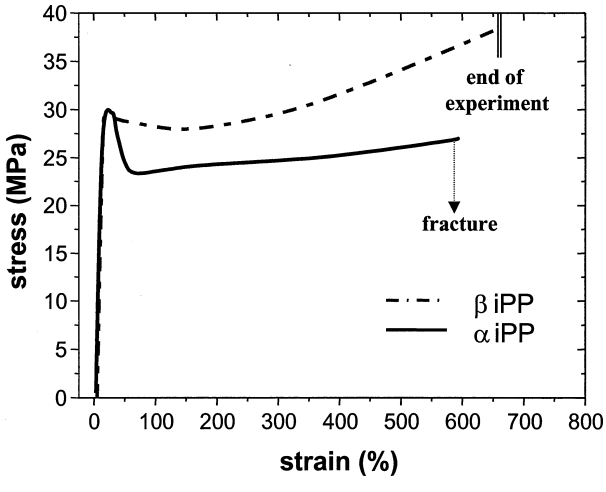

Figure 4 Stress-strain curves of α-iPP and β-iPP: the test was stopped for β-iPP before fracture.

3.1.3. Micromechanical processes

A typical micromechanical process of deformation of β-iPP is visible in Fig. 5 in a scanning electron micrograph of the deformed sample close to the necking region (for the starting morphology see Figs 2b and 3). Straining is in the horizontal direction (perpendicular to the direction of the lamellar stacks). For the initial stages of deformation ($\lambda \approx 1.2$), two main types of plastic processes can be distinguished: A formation of a chevron-like morphology (zig-zag pattern) due to collective twisting of lamellar stacks and a lamellar separation process are observed simultaneously. Whereas the former process does not include a change in sample volume, the latter is accompanied by intensive microvoid formation and fibrillation within the amorphous portion that can be interpreted as a craze-like deformation mechanism (see Fig. 6). From the measurement of average lamellar thickness we conclude that in the initial deformation stage represented here, the crystalline

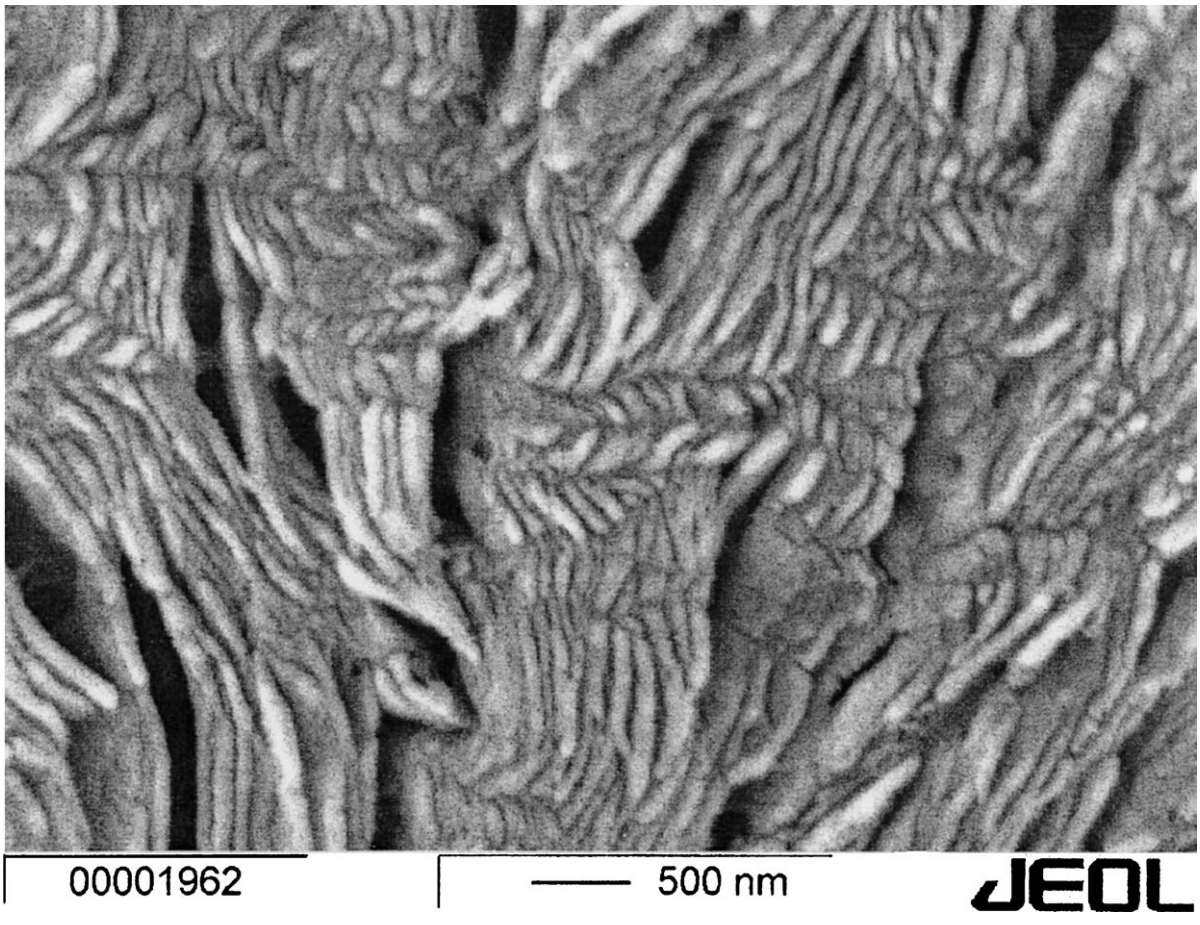

Figure 5 SEM micrograph showing deformation structures of lamellar separation and chevron formation in β-iPP; deformation direction is horizontal; SEM imaging after permanganate etching.

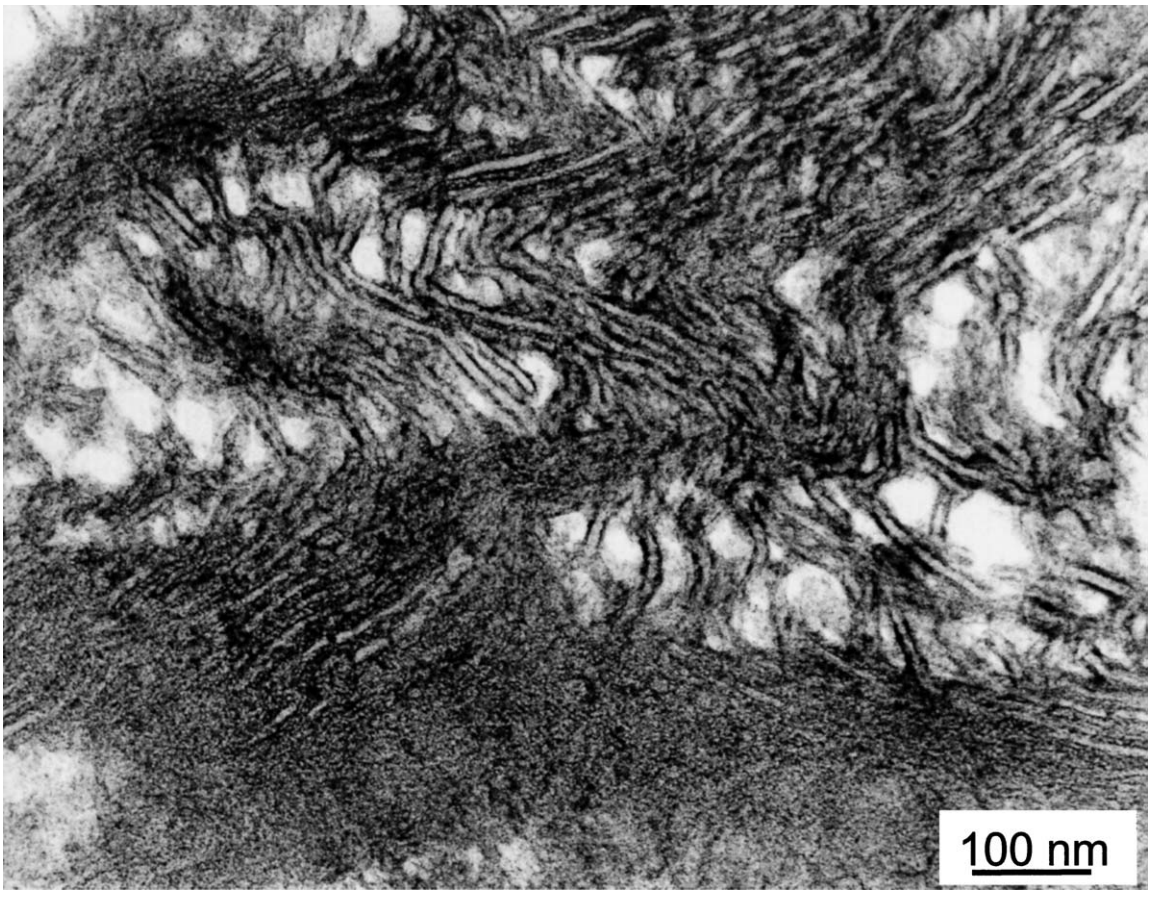

Figure 6 TEM micrograph showing details of deformation structures in the iPP; deformation direction is horizontal; RuO_4 staining causes the less denser amorphous phase appearing dark.

lamellae (appearing as white strands in Fig. 6) stay intact. The simultaneous process of chevron formation and lamellar separation are controlled by the mobility of the interlamellar, amorphous portion of the material.

3.1.4. Results from FTIR studies

Fig. 7 reveals the orientation behaviour of β-iPP chains in the crystalline and amorphous parts. Obviously, the average orientation of chains in the amorphous phase is much lower than that in the crystalline phase. It should be noted that the orientation of amorphous chains depends strongly on their conformation. For example, the tie chains, interconnecting the lamellae, can be oriented very strongly as a consequence of a high tensile stress in the stretching direction [21]. In contrast, chain ends cannot be oriented, and branches or short chains with low molecular weight are only slightly oriented.

The orientation behaviour of chains in the crystalline phase in the β-iPP samples is typical of semicrystalline polymers. At the initial stage of deformation, there is a decrease in the degree of orientation relative to the stretching direction, which again increases at higher deformation. Two steps of the molecular deformation mechanisms of iPP are discussed [19, 22]: the interlamellar slip at low deformation and the intralamellar slip. Thus, during uniaxial stretching the chain lamellae as stiff deformation units will be first twisted into the stretching direction resulting in a molecular orientation in the perpendicular direction because the folded chains are aligned in perpendicular direction to the lamellar axis. At higher elongation and when many of the lamellae are rotated into the direction of loading, the chains within the lamellae start to yield and will be oriented parallel to the stretching direction leading to an increase of the orientation degree. In principle, the orientation behaviour of chains in the crystalline phase in α- and β-iPP samples is similar. However, it was found that α-iPP discriminates the first deformation step (rotation or twisting of lamellae), whereas β-iPP favours the first step. Details about the molecular deformation behaviour of iPP were discussed elsewhere [19].

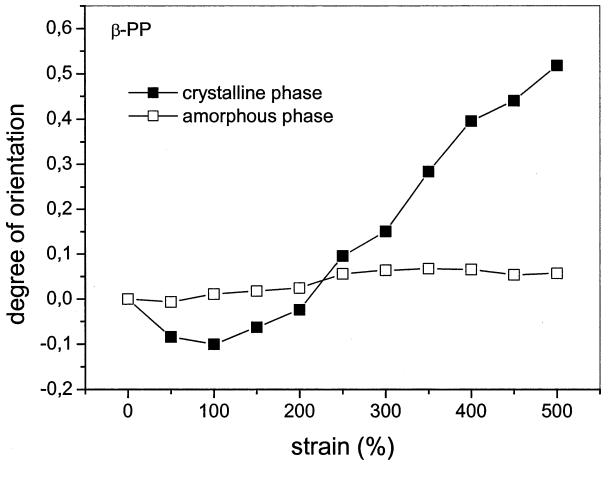

Figure 7 Degree of orientation as a function of applied strain determined by FTIR spectroscopy showing the selective orientation behaviour of crystalline and amorphous phases in β-iPP.

3.2. Morphology and micromechanical processes of lamellar SBS block copolymers

3.2.1. Morphology

TEM micrographs in Fig. 8 show the morphology of a highly asymmetric SBS triblock (Fig. 8a) and a star block copolymer (Fig. 8b). Both of them have a total styrene volume fraction of 0.74 and possess a tapered interface. The details of the morphology formation in these block copolymers may be found in [13, 23]. The linear triblock copolymer (SBS-Ln) possesses a clear lamellar morphology. The star block copolymer (SBS-St) reveals a more complex 'two-component three-phase morphology' consisting of alternating layers of polystyrene (PS) and polybutadiene (PB) with PB layers containing scattered polystyrene inclusions. The phase morphology of both of these block copolymers deviates significantly from the classical block copolymer phase diagram, which is a consequence of the modified molecular architecture. In a linear diblock copolymer with equivalent chemical composition PB cylinders in a PS matrix would be expected [7]. The PS lamella thickness and lamellar long period in these block copolymers lie in the range of 15–20 nm and 35–40 nm, respectively.

In Fig. 8b microdomains or grains are visible, which possess an internal local orientation, but they have no preferential orientation on a macroscopic scale. Such a morphology may be regarded as being macroscopically isotropic. Under the influence of an external field such as shearing or electric field, the microdomains in the block copolymers may be turned to possess nearly a monodomain structure (highly anisotropic morphology) [24, 25].

3.2.2. Mechanical properties

The modified molecular structure and microphase separated morphology result in a change in mechanical properties of the block copolymers. Fig. 9 compares the stress-strain curves of the lamellar triblock copolymer discussed in this work (morphology in Fig. 8a) with that of a symmetric SBS triblock copolymer having equivalent chemical composition. Compared with the symmetric block copolymer, the asymmetric sample has a lower yield stress and Young's modulus. However, the strain at break (ε_B), which is a measure of ductility of the polymers, is much higher for the asymmetric copolymers. The value of ε_B reaches up to about 450% compared to about 10% strain in the symmetric SBS copolymer. Consequently, the lamellar triblock (SBS-Ln) possesses a much higher toughness.

3.2.3. Micromechanical processes

The mechanical properties of the block copolymers can be discussed in the light of their micromechanical behaviour, i.e., by analysing the strain induced structural changes in the samples.

Fig. 10 shows the morphology of the star block copolymer (SBS-St) before and after tensile deformation. The microdomains were oriented by processing

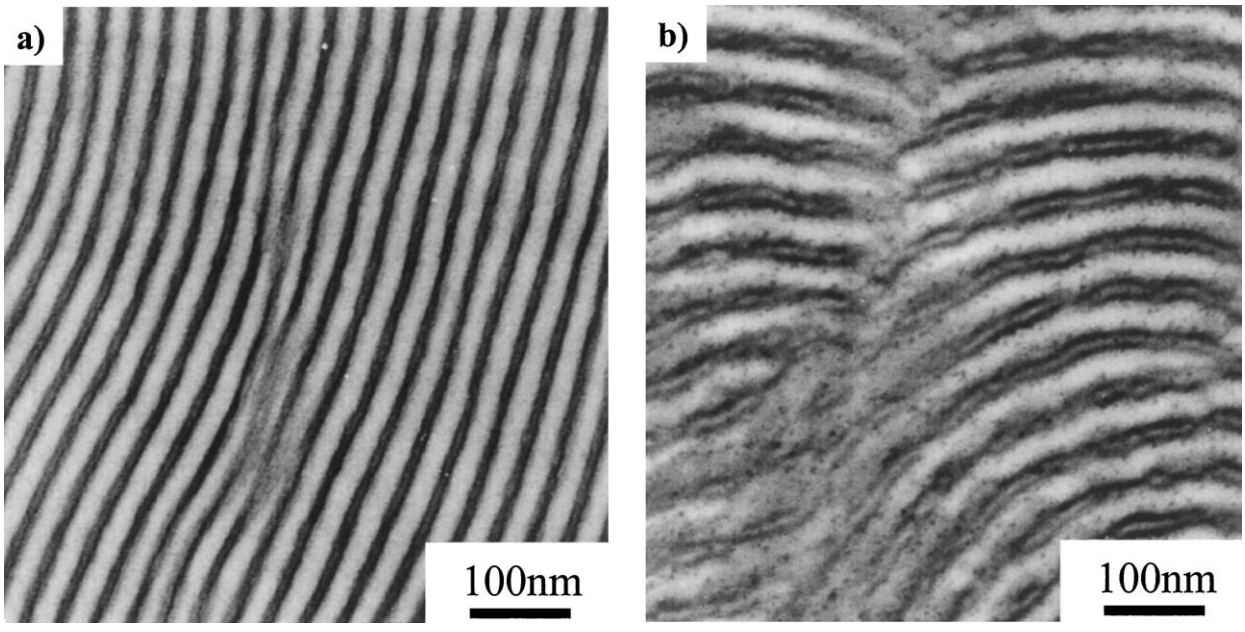

Figure 8 TEM micrographs showing the microphase separated morphology of the block copolymers in solution cast films, OsO_4 staining makes the butadiene phase appearing dark in the micrographs; (a) triblock copolymer and (b) star block copolymer.

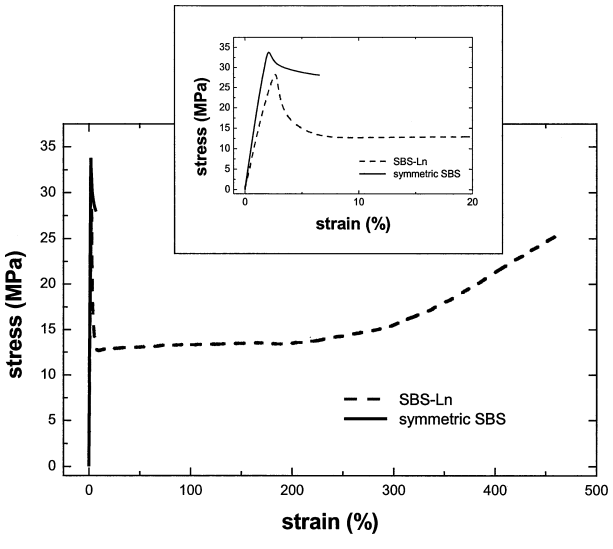

Figure 9 Stress-strain curves of the asymmetric triblock copolymer studied (SBS-Ln) compared with a symmetric triblock copolymer having identical chemical composition; tensile testing using injection moulds at 23°C according to ISO 527.

the sample by injection moulding. In the undeformed sample, the thickness of the PS lamellae and the lamellar spacing lie in the range of 20 and 42 nm, respectively (Fig. 10a). The tensile deformation parallel to the injection direction (i.e., the lamellar orientation direction) led to an extreme plastic drawing of both PS and PB lamellae (Fig. 10b). In the deformed sample the thickness of the PS lamellae and the lamellar spacing have been reduced to about half of their values before deformation. It is worth mentioning that the lamellae were stretched to a very high degree without any cavitation or microvoid formation. In contrast to the diblock copolymers, where a deformation localisation in the form of craze-like zones is the principal deformation mechanism [26, 27], no local deformation bands were observed.

From an analysis of the lamellar spacing and the thickness of the PS lamellae in the undeformed and deformed samples, one can estimate an elongation of the lamellae of about 300%; this is the same order of magnitude as maximum stretching of the entanglement network of PS and of the fibrils inside the crazes of homopolystyrene (with a maximum craze fibril extension ratio of $\lambda = 4$ [2, 28]). In other words, the yielding of the lamellae in the star block copolymer is analogous to the drawing of craze fibrils in the polystyrene homopolymer. The homogeneous yielding of PS lamellae (thin PS layers) together with adjacent PB ones can be described by a new deformation mechanism called *thin layer yielding* [29], which is schematically represented in Fig. 11. This effect appears if the thickness of the PS layers lies below a critical value (a critical thickness D_{crit}). This critical thickness is comparable to the maximum craze fibril thickness in polystyrene homopolymer, i.e., in the range of 20 nm. The difference between the craze fibril yielding and the yielding of the PS lamellae lies in the fact that the craze fibrils are stretched between microvoids while the PS lamellae undergo unconstrained yielding between PB lamellae. The PB lamellae may be regarded as being at the liquid-like state owing to its low glass transition temperature ($T_g \sim -60$°C in the present case) and do not hinder the plastic deformation of the glassy polystyrene layers. The covalent linkage of the polybutadiene chains at both the ends with the high T_g chains (i.e., the PS chains) restricts the void formation in the PB phase.

The large plastic deformation of the glassy lamellae at room temperature under tensile loading conditions was confirmed in several lamellar block copolymer systems. In particular, when the average thickness of the PS lamellae increases to about 30 nm, the deformation mechanisms changes from homogeneous drawing of the lamellae to the formation of local craze-like zones [30]. This finding provided an additional evidence for the '*thin layer yielding*' mechanism. The significance

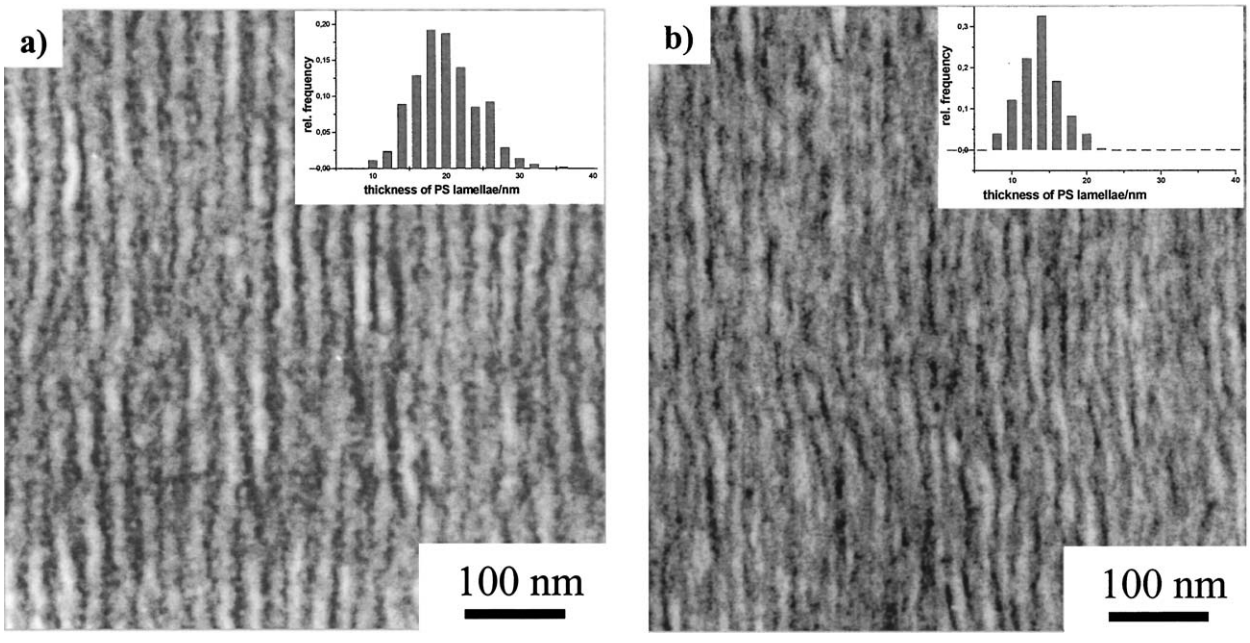

Figure 10 TEM micrographs showing the morphology of injection moulded star block copolymer (SBS-St): (a) before deformation and (b) after deformation; deformation direction is vertical, the distribution of the PS lamella thickness in the samples is shown in inset.

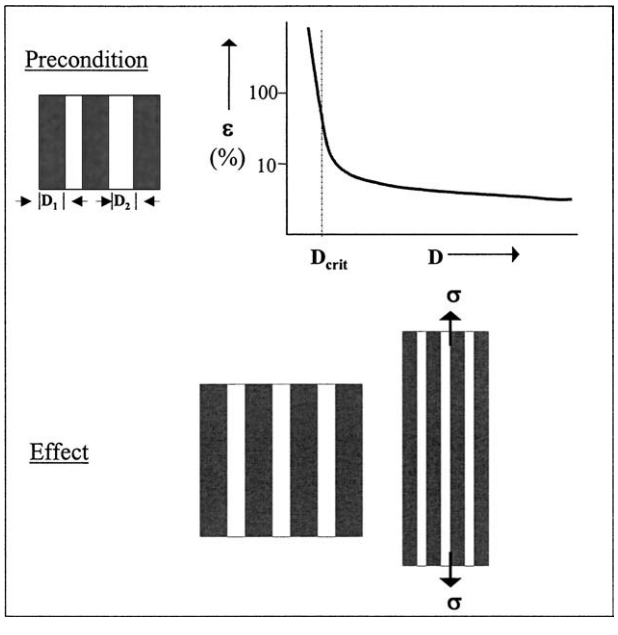

Figure 11 Scheme showing the principle of 'thin layer yielding' mechanism; D, D_c, and ε stand for PS layer thickness, critical layer thickness and elongation at break, respectively.

of this mechanism from the engineering point of view may be found in the fact that it can be used as an alternative toughening mechanism for brittle polymers [29].

If the material is loaded perpendicular or at an angle to the lamellar orientation direction, the lamellae break into shorter pieces which rotate into the deformation direction and are folded in a fish-bone-like arrangement (chevron morphology). The morphology of a lamellar triblock copolymer film (SBS-Ln) cast from solution is shown in the SFM phase images in Fig. 12. After deformation, the regions where lamellae were originally perpendicular to the strain direction turn into a so called 'chevron morphology' or fish-bone morphology (zig-zag pattern).

Detailed examination of deformation zones in the lamellar block copolymers demonstrate that the thickness of the PB layers and the lamellar spacing at the 'hinge' regions were larger than that in the 'limbs'. Moreover, the thickness reduction of the PB layers during the parallel deformation was found to be more pronounced. These observations indicate that the rubbery phase reacts earlier towards the applied stress than the PS phase, a result, which is also supported by FTIR results.

3.2.4. Results from FTIR studies

In Fig. 13 the selective orientation behaviour of a SBS triblock copolymer (SBS-Ln) is shown. At the initial stage of deformation of the butadiene chains orient earlier and stronger than the styrene chains. Above approximately 50% strain the styrene chains orient significantly with increasing strain. In contrast, at this deformation stage, the orientation of PB chains shows a smaller increase with strain, indicating that the applied stress is transferred more and more into the hard phase. In connection with morphological investigations by means of SFM, the SBS block copolymer deforms with a two step mechanism, discussed in detail in [31]: At the beginning of deformation the higher mobility of the PB phase enable slipping and rotation of the PS lamellae with an increasing degree of orientation in the soft phase. At larger deformations the lamellae, which are more or less oriented in deformation direction, start to yield (thin layer yielding) with increasing orientation in the hard phase.

4. Discussion

4.1. Influence of morphology

It has been found that similar micromechanisms appear in two entirely different classes of materials, which are

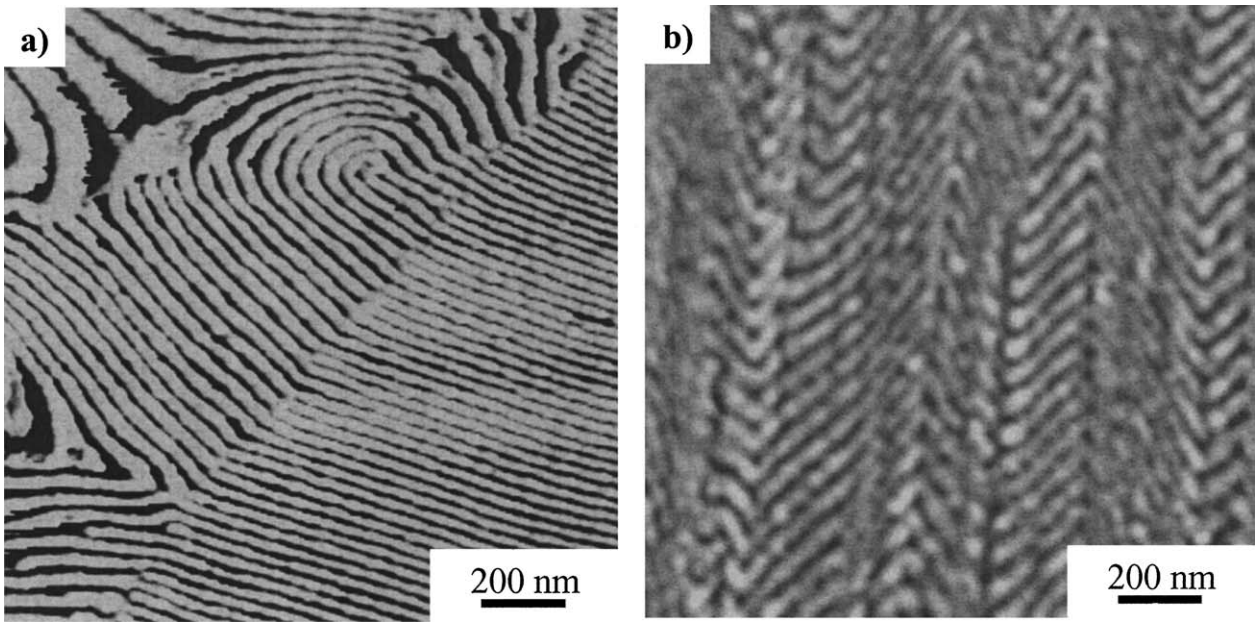

Figure 12 Tapping mode SFM images of the triblock copolymer (SBS-Ln): (a) before deformation and (b) after deformation; deformation direction is vertical, PB phase appears dark.

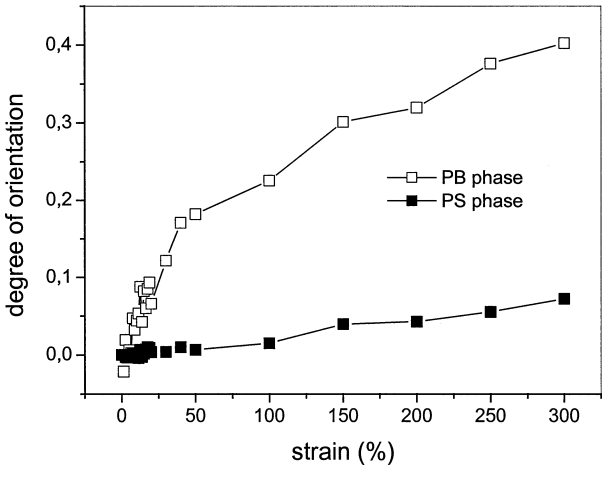

Figure 13 Diagram of orientation function versus strain measured by FTIR spectroscopy on the lamellar triblock copolymer (SBS-Ln).

responsible for the observed ductility of the polymers studied and which result from their comparable morphology (see Fig. 1 and Table II).

Depending on the loading direction relative to the lamellar alignment, different processes of deformation exist as shown schematically in Fig. 14. In the semicrystalline polymers, during loading parallel to the lamellar orientation direction (in Fig. 14 left), slippage of lamellae is followed by breaking of lamellae into smaller fragments and separation of the crystallites. Chain unfolding occurs in the crystals leading to the formation of microfibrils at very high deformations. In the lamellar block copolymers slippage of lamellae is followed by the dominating mechanism of 'thin layer yielding'. These processes are associated with successive orientation of the macromolecules towards the deformation direction as demonstrated by the FTIR measurements.

When loading perpendicular to the lamellar orientation direction (in Fig. 14 right), similar deformation structures are formed both in β-iPP and lamellar SBS block copolymers—separation of lamellae and formation of chevron morphology. Additionally, in β-iPP cavitation and fibrillation in the amorphous phase appear. At high deformations, if fragments of lamellae are oriented into the deformation direction, microfibril formation or thin layer yielding start.

The absence of microvoids in the soft phase of the SBS block copolymers is a most striking difference (see Fig. 15). The butadiene phase covalently bonded to the styrene chains is free of molecular defects and would allow cavitation only after chain scission. In iPP the amorphous region contains a number of defects (such as chain ends or weak entanglements) yielding to cavitation during lamellar separation and to the formation of craze-like structures (in the top of Fig. 15). The high plastic deformation of the amorphous region (including the formation of fibrillated crazes) in iPP leads to a

TABLE II Summary of the micromechanisms of the investigated systems

	Micromechanism observed in	
Loading direction	β-iPP	Block copolymer
$\parallel$	Separation of crystal blocks, fragmentation, unfolding of crystals	Shearing of rubbery layers, yielding of PS lamellae
$\perp$	Lamellar separation, cavitation and fibrillation in the amorphous region, chevron formation	Shearing of rubbery layers, chevron morphology formation, no cavitation

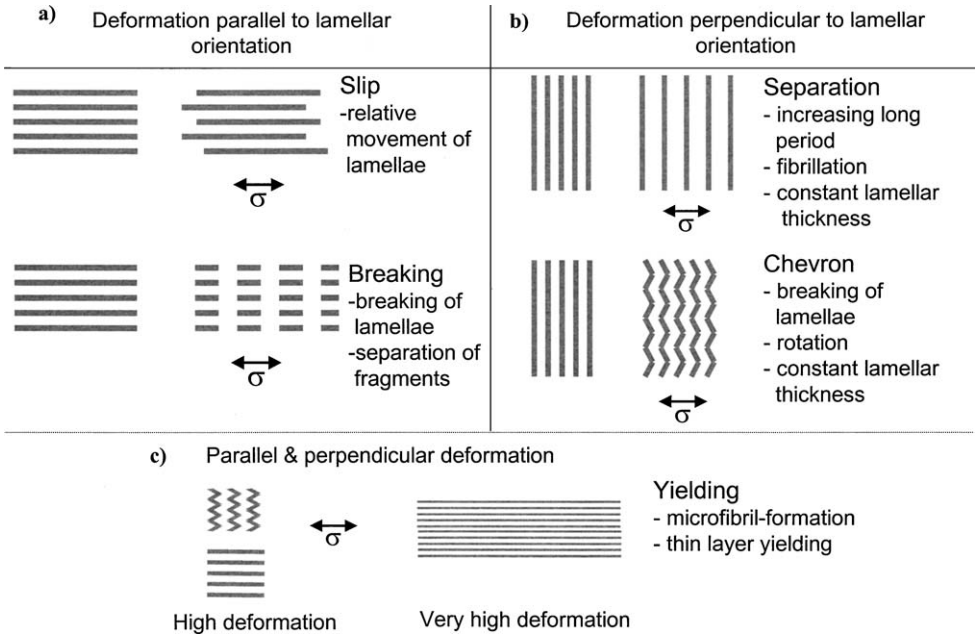

Figure 14 Scheme of micromechanical processes observed in lamellar systems investigated: lamellae parallel to the strain direction (left) and lamellae perpendicular to the strain direction (right).

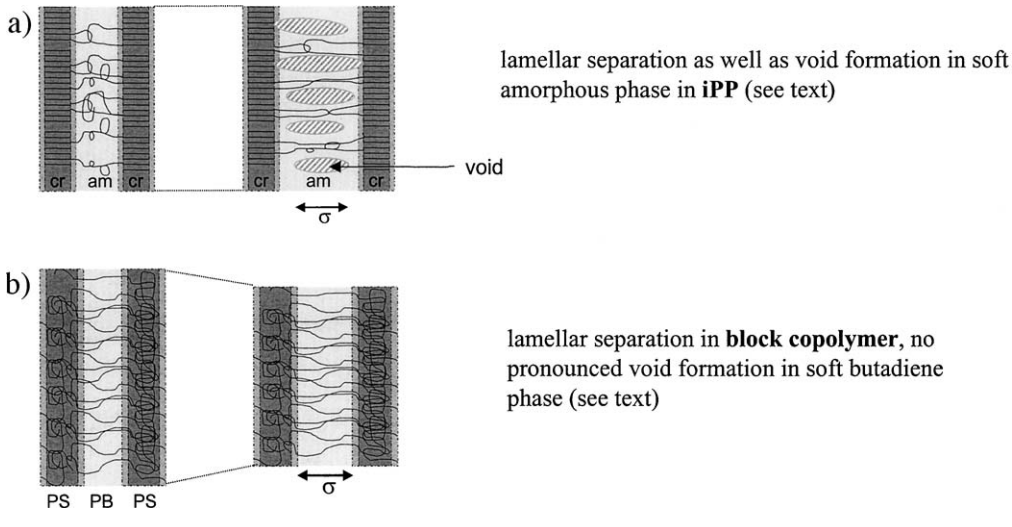

Figure 15 Scheme showing the deformation of the soft lamellae if they are aligned perpendicular to the strain direction: (a) stretching with void formation in the soft amorphous phase in β-iPP and (b) stretching without void formation in the rubber phase of SBS block copolymer.

high ductility of this sample. Therefore, the toughness in the β-form of iPP is greater than that of the α form (in α-iPP the plastic deformation in the amorphous region is hindered due to the cross-hatched morphology).

4.2. Influence of T_g

The stiffness of an amorphous polymer is controlled by its glass transition temperature (T_g). The decisive role in the initial stage of deformation is played by the low T_g (or softer) component, which, owing to its low Young's modulus, starts to deform plastically and initiates slippage or separation of the neighbouring hard phase (lamellae). After transformation of larger stresses to the hard components, these start to yield plastically.

In both the polymers investigated, the T_g of the soft component (T_{g-soft}) is well below the test temperature (T_g of the amorphous phase in iPP and T_g of the butadiene phase in the block copolymer; see Table III). That means, there is a large value of ΔT (the T_g difference in the block copolymer or the difference between melting point T_m and T_g in iPP), which may be regarded as being a reason of the extreme plastic deformation of both the hard and soft components. Results from the literature show that a large ΔT could act as a precondition for high ductility in lamellar systems. In a styrene/methyl

TABLE III Glass transition temperatures and melting temperatures of the investigated polymers

	Polymer	
Properties	β-iPP	SBS block copolymer
$T_{g-soft}(T1)/^\circ C$	-5	~ -60
$T_{m-crystal;}T_{g-hard}(T2)/^\circ C$	165	$+100$
$\Delta T = T2 - T1/^\circ C$	170	160

methacrylate block copolymer, none of the components is soft at room temperature, and the glass transition temperatures of the phases are not widely separated (ΔT = ca. 10°C). It leads to the formation of crazes even if the microphase separated morphology is made up of lamellae [32]. Likewise, in the very brittle syndiotactic polystyrene the high $T_g \sim 100$°C of the amorphous parts between the crystalline lamellae is far above the test temperature and prevent a ductile deformation [33].

4.3. Discussion of maximum elongation

It is to be noted that, in spite of the existence of similar deformation mechanisms, β-iPP and SBS block copolymers show a great difference in ductility. While β-iPP reaches an elongation of over 600% up to break (ε_B), lamellar SBS block copolymers show a much smaller value (about 300%). This effect may be explained due to two effects.

The maximum elongation achieved by the block copolymer is contributed by the stretching of the rubbery network and that of the polystyrene phase. The draw ratio of the rubbery network might be very high but it is restricted by the glassy polystyrene lamellae, which act as physical cross-links. The maximum stretching of the PS is limited by the draw ratio of the entanglement network, which is equal to about 4 ($\lambda_{max} = 4$ or 300% strain). This value is the limit of the thin layer yielding mechanism and is realised in the crazes in bulk polystyrene [2, 28].

In the lamellar iPP, the interlamellar amorphous region is also a network of entangled chains, whose stretching is again limited by the neighbouring crystalline lamellae. However, the cavitation in the amorphous region allows the higher contribution of the soft phase to the macroscopic strain. Another contribution comes from the conversion of folded macromolecular chains inside the lamellae into the microfibrils; it can be roughly estimated that the chain unfolding in the crystalline phase may even result in an elongation as high as $\lambda_{max} > 100$. At room temperature (23°C in our case), the molecular mobility is limited and this maximum elongation cannot be realised. Values close to λ_{max} have been realised in crystalline polymers (e.g., polyethylene, polypropylene) by the use of special techniques, e.g., gel casting, solution drawing etc. [34].

5. Concluding remarks

Two entirely different classes of lamellae forming heterophase polymers (semicrystalline β-iPP and amorphous styrene/butadiene block copolymer) are found to deform via a similar micromechanical mechanism. It is concluded that the reason is a similar nanostructured lamellar polymeric system with soft and hard components. The basic mechanisms show two stages. The initial stage is characterised by a plastic deformation of the soft phase with a reorganisation and an alignment of the hard (glassy or crystalline) lamellae towards the deformation direction. The second one is determined by the plastic yielding of the hard lamellae due to thin layer yielding (SBS block copolymer) or unfolding (iPP). In this way, the knowledge of deformation processes of one type of polymers may be used to understand better the deformation mechanism of another type of polymer having comparable phase morphology, even though they consist of different types of macromolecules.

Acknowledgements

This work is funded by the Deutsche Forschungsgemeinschaft and the Kultusministerium des Landes Sachsen-Anhalt. Financial support from the Deutscher Akademischer Austauschdienst (DAAD) and from the Alexander von Humboldt (AvH)-Stiftung are acknowledged. Research scholarships from the Max-Buchner-Forschungsstiftung (MBFSt 6052 for R.A. and MBFSt 2280 for S.H.) are thankfully acknowledged. We further extend our thanks to BASF Aktiengesellschaft, Ludwigshafen and Borealis Aktiengesellschaft, Linz for the supply of materials. We are indebted to Mrs. S. Goerlitz for the TEM investigations, Dr.T.A. Huy for providing the FTIR results, and Prof. W. Grellmann and Mrs. S. Ilisch for the possibility of tensile testing.

References

1. G. H. MICHLER, Deformation and Fracture (Micromechanical Mechanisms), in "Polymeric Materials Encyclopedia," edited by J. S. Salamone (CRC Press, New York, 1996) p. 1771.
2. *Idem.,*"Kunststoff-Mikromechanik: Morphologie, Deformations- und Bruchmechanismen" (Carl Hanser, München, 1992).
3. M. RÄTZSCH, *Kunststoffe* **88** (1998) 8.
4. J. KARGER-KOCSIS and J. VARGA, *J. Appl. Polym. Sci.* **62** (1996) 291.
5. J. KARGER-KOCSIS, *Polym. Eng. Sci.* **36** (1996) 203.
6. G. HOLDEN, "Understanding Thermoplastic Elastomers" (Carl Hanser, Munich, 2000).
7. I. W. HAMLEY, "The Physics of Block Copolymers" (Oxford Science Publishers, London, 1998).
8. F. S. BATES and G. H. FREDRICKSON, *Phys. Today* **2** (1999) 32.
9. V. ABETZ and T. GOLDACKER, *Macromol. Rapid Comm.* **21** (2000) 16.
10. K. KNOLL and N. NISSSNER, *Macromol. Symp.* **132** (1998) 231.
11. C. LEE, S. P. GIDO, Y. POULOS, N. HASDICHRISTIDIS, N. B. TAN, S. F. TREVINO and J. W. MAYS, *J. Chem. Phys.* **107** (1997) 6470.
12. S. T. MILNER,*Macromolecules* **27** (1994) 2333.
13. R. ADHIKARI, G. H. MICHLER, T. A. HUY, E. IVANKOVA, R. GODEHARDT, W. LEBEK and K. KNOLL, *Macromol. Chem. Phys.* **204** (2003) 488.
14. R. OLLEY, D. C. BASSET, P. J. HINE and I. M. WARD, *J. Mater. Sci.* **28** (1993) 1107.
15. H. W. SIESLER and K. HOLLAND-MORITZ, "Infrared and Raman Spectroscopy of Polymers" (Marcel Dekker Inc, New York and Basel, 1980).
16. H. W. SIESLER, in "Oriented Polymer Materials," edited by S. Fakirov (Hüthig & Wepf Verlag, Heidelberg, 1996) Chapt. 4, p. 138.
17. T. A. HUY,"Rheo-Optische Charakterisierung des Deformationsverhaltens Dynamischer Vulkanisate" (Shaker Verlag, Aachen, 1999).
18. M. HOUSKA,*Polym. Eng. Sci.* **27** (1987) 917.
19. T. A. HUY, T. LUEPKE, S. HENNING and G. H. MICHLER, *J. Polym. Sci., Polymer Phys.*, submitted.
20. R. A. PHILLIPS and M. D. WOLKOWITCZ, in "Polypropylene Hand Book," edited by E.P. Moore, Jr. (Carl Hanser Verlag, Munich, 1996) p. 113.
21. V. PETRACCONE, I. C. SANCHEZ and R. S. STEIN, *J. Polym. Sci., Polymer. Phys. Ed.* **13** (1987) 917.

22. T. A. HUY, T. LUEPKE and H.-J. RADUSCH, *J. Appl. Polymer. Sci.* **80** (2001) 148.24.
23. R. ADHIKARI, R. GODEHARDT, W. LEBEK, R. WEIDISCH, G. H. MICHLER and K. KNOLL, *J. Macromol. Sci.* B **40** (2001) 833.
24. Y. COHEN, R. J. ALBALAK, B. J. DAIR, M. S. CAPEL and E. L. THOMAS, *Macromolecules* **33** (2000) 6502.
25. C. C. HONEKER, E. L. THOMAS, R. J. ALBALAK, D. A. HADJUK, S. M. GRUNER and M. C. CAPEL, *ibid.* **39** (2000) 9395.
26. C. E. SCHWIER, A. S. ARGON and R. E. COHEN, *Polymer* **26** (1985) 1985.
27. R. WEIDISCH and G. H. MICHLER, in "Block Copolymers," edited by F. J. Baltá-Calleja and Z. Roslaniec (Marcel Dekker, New York, 2000) p. 215.
28. E. J. KRAMER, in "Advances in Polymer Science: 52/53, Crazing in Polymers-Vol I," edited by H.H. Kausch (Springer Verlag, Berlin, Heidelberg, 1983) p. 5.
29. G. H. MICHLER, R. ADHIKARI, W. LEBEK, S. GOERLITZ, R. WEIDISCH and K. KNOLL, *J. Appl. Polym. Sci.* **85** (2002) 683.
30. R. ADHIKARI, G. H. MICHLER, S. GOERLITZ and K. KNOLL, *ibid.* **92** (2004) 1208.
31. T. A. HUY, R. ADHIKARI and G. H. MICHLER, *Polymer* **44** (2003) 1247.
32. C. CRETON, E. J. KRAMER and G. HADJIIONNAU, *Coll. Polym. Sci.* **270** (1992) 399.
33. F. RAMSTEINER, G. E. McKEE, W. HECKMANN, S. OEPEN and M. GEPRÄGS, *Polymer* **41** (2000) 6635.
34. M. MATSUO, in "Oriented Polymer Materials," edited by S. Fakirov (Hüthig & Wepf Verlag, Heidelberg, 1996) Chapt. 10, p. 303.

Received 6 January
and accepted 5 February 2004